PHYSICAL REVIEW B VOLUME 43, NUMBER 11 15 APRIL 1991-I

Electronic properties of the Penrose lattice. II. Conductance at zero temperature

Hirokazu Tsunetsugu
Institute for Solid State Physics, University of Tokyo, Tokyo 106, Japan

Kazuo Ueda
Institute of Materials Science, University of Tsukuba, Tsukuba, Ibaraki, Japan
(Received 21 June 1990)

The conductance of the Penrose lattice at zero temperature is studied by the multichannel Landauer formula and the recursion method of the site Green functions. We have investigated the dependence on the Fermi energy and the lattice size. The Fermi-energy dependence of the conductance studied for a system with up to 3571 sites exhibits singularly rapid and large conductance fluctuation. Analysis of system-size dependence of the fluctuations with respect to energy suggests the wave functions are critical. This critical behavior of the wave functions is more directly confirmed by the lattice length dependence, which shows power-law decays of conductance up to a system with about 1.32 million sites.

I. INTRODUCTION

In this paper we will study conductance of the Penrose lattices (PL) at zero temperature following the preceding paper[1] (hereafter referred to as I), where we studied the electronic structure of the same model. As discussed in Paper I, the electronic structures of quasicrystals (QC) show singular behaviors that originate from their quasiperiodic lattice structures. Our conclusion on the PL was that the energy spectrum has a singular part but the total bandwidth remains finite and most of the wave functions are localized in a power law.[2] It is quantum transport properties such as conductance that reflect the singular electronic structures most clearly, because the conductance is a site off-diagonal quantity and hence sensitive not only to amplitude of the wave functions but also to their phases. Besides, conductance is in itself an intriguing and important property which characterizes various kinds of condensed matter. Therefore we expect that the electronic properties and transport properties of QC become clearer through the calculation of conductance of the PL. Unsmoothness of the density of states (DOS) would lead to singular energy dependence of the conductance,[3] and the localized nature of the wave function influences its system-size dependence.[4,5]

A singular behavior of conductance in the PL was also pointed out by Choy,[6] but the systems he used were not large and the use of a finite imaginary part for energy variable in the Green functions was unavoidable in numerical computations. The above two facts made it difficult to observe such intrinsic character, because the finite imaginary part as well as finite temperatures smears out quantum coherence of the wave functions; singular electronic properties of QC, however, originate from the interference effect of the coherent wave functions. Sokoloff treated the transport properties of QC by applying the Faber-Ziman scheme to the scattering time of electron propagation.[7] He stated that the quasiperiodic structures yield no singular scattering and suggested the existence of another origin of high resistivity observed in real QC alloys. The Faber-Ziman formula was originally developed for liquid metals and determines the scattering time by the Born scattering process caused by the weak pseudopotential. Through the study of the Anderson localization problem, however, it has become clear that essential to this problem is the correlation between two one-particle Green functions in the response function and also that, beyond the Born approximation, the quantum coherence effect should be carefully taken into account. Hence direct calculation without such approximations is necessary for the question of whether QC have intrinsic singular transport properties characteristic to their quasiperiodic structures. In order to investigate such intrinsic character in detail, we will calculate the dependence of the conductance on the Fermi energy and on the lattice length at zero temperature for the systems as large as possible, using the multichannel Landauer formula,[8] which is free from the artificial imaginary part of energy variables. The results will be discussed based on the electronic structure studied in Paper I.

Conductance of a one-dimensional QC, the Fibonacci chain (FC), has been studied in great detail by many researchers.[9,10] One advantage of the model is that analytical treatments are available, since the 2×2 transfer matrices, which determine the conductance, obey a simple dynamical mapping. In particular, Sutherland and Kohomoto showed that increase in the resistance with the system size is bounded by a power-law function and that the distribution of resistance values has a multifractal character at energies within the spectrum where the trace map tends to a limit cycle.[10] As is expected, conductivity is not a well-defined quantity in this model. As an example, Goda showed the resistance changes the lattice length dependence from power-law increase to exponential increase at the energies within energy gaps.[11] These unusual behaviors of the FC model directly reflect the character of its wave functions.

It is much more difficult to study conductance of the

PL than the FC because no analytical treatments are available. But since the FC is rather a special model in the QC family as discussed in Paper I, the study of QC in higher dimensions is indispensable for deeper understanding of characteristic behaviors of their transport properties. In this connection, it is worthwhile to note that there are some essential differences between the FC and the PL. One is the difference of the energy spectrum. The results in Paper I showed that the PL has an energy spectrum including a singular part but the total bandwidth remains finite. On the other hand, the spectrum of the FC is a Cantor set and the total bandwidth is always zero no matter how small the quasiperiodic potential (or transfer) is.[12] Another important difference is the dimensionality itself. In one dimension the length dependence of conductance is completely determined by the spatial form of the eigenstate wave function at the Fermi energy. But in higher dimensions, since multiple eigenstates are degenerate at a fixed energy, conductance is not dominated only by localization behavior of each eigenstate, and mode mixing between them plays an important role.[13]

This paper is organized as follows. In Sec. II, we explain our method of numerical computations. In Secs. III and IV, we show the results of numerical computations of the Fermi-energy dependence and the lattice length dependence, respectively, and discuss the results. Section V is devoted to conclusions. Some results of this work have been published in short notes.[3–5] In this paper we present our results in more systematic form and discuss them from various aspects.

II. METHOD OF CALCULATION

In this section, we explain our method of calculating conductance of the PL. In general, care is necessary in the proper definition of the conductance of finite systems. As the definition of conductance, we apply the multichannel Landauer formula[8] (MCLF) originally developed in the Anderson localization problem, because in this formula there is no ambiguity in defining conductance even for finite systems. The reason for giving finite conductance is that the MCLF defines conductance in a configuration where the relevant finite system is connected to two lead lines of infinite length, and consequently the total system has a continuous energy spectrum. In the original formula by Anderson *et al.*, the MCLF defines conductance by the scattering matrix in this configuration; later Lee and Fisher[14] rewrote the formula in terms of the site Green functions, which proved effective in calculating length dependence. But to apply the Lee-Fisher expression to our case, several modifications are necessary, since the PL is topologically nonperiodic. We would like to point out that another efficient scheme—the transfer-matrix method[13,15]—cannot be applied to the PL. This is due to the existence of a special scattering mechanism in QC. We will return to this point at the end of Sec. IV. In contrast, with random potentials on a regular lattice, careful selection of a pattern of PL as a scatterer is needed in order to reduce undesirable scattering originating from the scatterer boundaries and the interfaces to the lead lines, which scattering would smear out intrinsic transport properties otherwise. The periodic approximations of the PL used in Paper I are appropriate for this purpose because we can reduce the surface scattering by imposing the periodic boundary condition in the lateral direction of electric current. We will use unit cells of the periodic Penrose lattices[1,2] (PPL) as scatterers to study energy dependence because we have already studied their electronic structures, but the semiperiodic Penrose lattices[1,4] (SPPL) are more suitable for studying length dependence because they hold quasiperiodicity in the current direction.

We show an example of our configuration of the MCLF in Fig. 1. The central part is a relevant scatterer, i.e., a unit cell of a PPL or a finite section of a SPPL, and the left and right parts are lead lines—square lattices with infinite length and finite width M. We use the same model as Paper I; put atoms in the *center* of each rhombus (or square in the lead lines) and set the electron transfer energy to be -1 only for nearest-neighbor pairs. The distortion at the interfaces between the scatterer and the lead lines is of no significance, because our choice of the transfer energies does not depend on the distances of atoms but only on the connectivity.

First, we explain the application of the original MCLF to the PL, which is used in calculating energy dependence of conductance. Later, we will explain the Lee-Fisher method used for the length dependence.

A. Direct method

The MCLF defines conductance as follows.[8] In the configuration where the scattering boundary condition is imposed to the lead lines, the amplitudes of the scattering waves $\mathbf{b}$ are related to the incident wave amplitudes $\mathbf{a}$ through the scattering matrix S, which describes the scattering processes by the scatterer:

$$\begin{bmatrix} \mathbf{b}_L \\ \mathbf{b}_R \end{bmatrix} = S \begin{bmatrix} \mathbf{a}_L \\ \mathbf{a}_R \end{bmatrix} = \begin{bmatrix} \mathbf{t} & \mathbf{r}' \\ \mathbf{r} & \mathbf{t}' \end{bmatrix} \begin{bmatrix} \mathbf{a}_L \\ \mathbf{a}_R \end{bmatrix}, \tag{2.1}$$

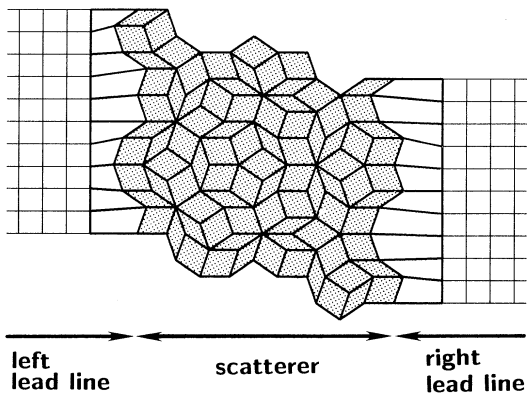

FIG. 1. Configuration of the MCLF. The shaded central part is the scatterer and a unit cell of the PPL is shown. (The right end column is attached to make the interface regular.) Lead lines are attached on both sides. The periodic boundary condition is imposed in the vertical direction and the system then has a cylindrical shape.

where $\mathbf{t},\mathbf{t}'$ are the transmission matrices, $\mathbf{r},\mathbf{r}'$ are the reflection matrices, and the subscripts L,R refer to the left and right lead lines. Conductance is defined in units of e^2/h per spin by[8]

$$g=\mathrm{Tr}(\mathbf{t}^\dagger\mathbf{t})=\sum_{\alpha,\beta}|t_{\alpha\beta}|^2 , \tag{2.2}$$

where $t_{\alpha\beta}$ is the transmission coefficient from the β channel in the left lead line to the α channel in the right lead at a specified Fermi energy E. The unitarity of the scattering matrix ensures that replacing $\mathbf{t}$ with $\mathbf{t}'$ in the defintion (2.2) does not change the result. Somewhat different definitions were also proposed[16] in addition to Eq. (2.2), but we will use the simplest definition (2.2) in this paper because we are interested in global behaviors of conductance with respect to the Fermi energy and the system size rather than in absolute values. In low-conductance cases such as our model, differences among various definitions are generally small quantitively. One advantage of the formula (2.2) is its high symmetry, e.g., it is invariant under unitary transformation of the channels.

We comment on our choice of channels. For a specified energy E, we choose plane waves in the lead lines as the channels and identify them by their momentums:

$$\psi_{\mathbf{k}}=e^{i\mathbf{k}\cdot\mathbf{r}}/\sqrt{2|\sin k_x|} , \tag{2.3a}$$

$$E=-2(\cos k_x+\cos k_y) ,$$

$$k_y=\frac{2\pi}{M}l \quad (l=0,\ldots,M-1) , \tag{2.3b}$$

where the subscripts x and y denote the directions parallel and perpendicular to the electric current respectively, M is the width of the lead lines, and the values of k_y are determined under the periodic boundary condition. The wave functions (2.3a) are normalized so that the total current of probability density should be unity in the x direction, which normalization leads to the unitarity of the scattering matrix. Note that the scattering matrix is defined between *propagating* waves **a** and **b** in the relation (2.1) and that their dimensions depend on the energy E. The propagating waves are given by real momenta k_x determined by Eq. (2.3b), while the other complex solutions correspond to exponentially decaying or increasing waves. Hereafter, we refer to them as *open channels* and *closed channels,* respectively. In the open channels the right going waves (incident waves in the left line $\psi^{\mathrm{in}}_{\mathbf{k}L}$ and scattering waves in the right lead line $\psi^{\mathrm{out}}_{\mathbf{k}R}$) have momenta $0<k_x<\pi$, and the left going waves (scattering waves in the left $\psi^{\mathrm{out}}_{\mathbf{k}L}$ and incident waves in the right $\psi^{\mathrm{in}}_{\mathbf{k}R}$) have momenta $\pi<k_x<2\pi$.

The scattering matrix can be obtained by solving a Schrödinger equation with the scattering boundary condition. Let the wave function at a specific energy E be expanded as follows in three regions,

$$\psi=\begin{cases}\displaystyle\sum_{\alpha=1}^{M_0}(\alpha_{L\alpha}\psi^{\mathrm{in}}_{\mathbf{k}_\alpha L}+b_{L\alpha}\psi^{\mathrm{out}}_{\mathbf{k}_\alpha L})+\sum_{b=1}^{M-M_0}c_{Lb}\phi_{Lb} & \text{(in the left lead line)}\\ \displaystyle\sum_{j}^{N}a_j\psi_j & \text{(in the scatterer)}\\ \displaystyle\sum_{\alpha=1}^{M_0}(a_{R\alpha}\psi^{\mathrm{in}}_{\mathbf{k}\alpha}+b_{R\alpha}\psi^{\mathrm{out}}_{\mathbf{k}_\alpha R})+\sum_{b=1}^{M-M_0}c_{Rb}\phi_{Rb} & \text{(in the right lead line)} ,\end{cases} \tag{2.4}$$

where ψ_j are atomic orbitals located at rhombus centers in the PL, and ϕ_{Lb},ϕ_{Rb} are wave functions exponentially decaying outwards in the lead lines. M_0 is the number of open channels and N is the site number in the scatterer part. The phases of the incident and scattering waves $\psi^{\mathrm{in}},\psi^{\mathrm{out}}$ can be set arbitrarily, and the scattering matrix will be transformed by the corresponding unitary matrix, but the observable quantity g is invariant under the transformation. Note that $\psi^{\mathrm{in}},\psi^{\mathrm{out}},\phi$ are determined from Eq. (2.3) for the specified energy E and the normalization of ϕ is irrelevant to the result of g. The Schrödinger equation to solve is

$$H\psi=E\psi , \tag{2.5}$$

for given incident wave amplitudes $\{b_L\}$ and $\{b_R\}$, and unknown variables are $\{a_L\}$, $\{a_R\}$, $\{c_L\}$, $\{c_R\}$, and $\{a_j\}$. Equation (2.5) is automatically satisfied in the lead lines except the sites adjacent to the scatterer, because electron transfer is limited to between nearest-neighbor sites. Therefore we have only to solve the Schrödinger equation (2.5) at the scatterer sites and the lead line sites adjacent to the scatterer. The number of both unknown variables and independent equations is $N+2M$, where N is the site number in the scatterer and the M is the lattice width (the total channel number including open and closed channels), and, consequently, we can determine $\{a_L\}$, $\{a_R\}$, $\{c_L\}$, $\{c_R\}$, and $\{a_j\}$ uniquely. The only exceptional case is when there are eigenstates confined within the scatterer at the specified energy, such as the confined states at $E=2.0$ in our model.[17] Even in that case, although $\{a_j\}$ are not unique, the scattering wave amplitudes $\{a_L\}$ and $\{a_R\}$ are uniquely determined. The scattering matrix is obtained by solving the Schrödinger equation for $2M_0$ incident waves. But for calculation of the conductance g, solutions for the M_0 right going incident waves are sufficient.

B. Recursion method

Next, we explain the recursion method for the MCLF modified from the original one for application to the PL. This method is efficient particularly for studying length dependence of conductance at a specified Fermi energy.

Lee and Fisher rewrote the formula (2.2) and obtained the expression given by the site Green functions in the same configuration[14]

$$g = 4\,\mathrm{Tr}[G''(L,L)G''(L+1,L+1) - G''(L,L+1)^2] , \tag{2.6}$$

where the double primes denote the imaginary part. The Green functions are defined at an energy including an infinitesimal imaginary part. The arguments of G refer to the coordinates in the current direction and G is still a matrix with respect to the lateral dimensions:

$$(G(L,L'))_{jj'} = \left\langle Lj \left| \frac{1}{E - i0 - H} \right| L'j' \right\rangle . \tag{2.7}$$

The conservation law of electric current ensures that the result (2.6) does not depend on the coordinate L in the current direction. But the natural choice of L is the one in the lead lines rather than in the scatterer, since the total current parallel to the current direction is defined easily; therefore, we will use the formula setting L in the right lead line. An advantage of the expression (2.6) is that we can calculate site Green functions efficiently using a recursion method.

We can simply specify the coordinate in the current direction as follows, in spite of nonperiodic lattice structure of the scatterer. The rhombus configuration in our scatterer (PPL or SPPL) is topologically the same as a pentagrid, so we can classify rhombuses into two groups by reference to the grid that repeats in the current direction (hereafter we will refer to it as the *0 grid*). One group is the rhombuses sitting on the 0 grid which form quasiperiodically spaced segments made of the same number of rhombuses (say the *0 grid segments*); the other is an ensemble of all other rhombuses, which are separated by the 0-grid segments, and we may consider them as glue that connects the 0-grid segments. We will thereby give the same coordinate l to each 0-grid segment or glue part (see Fig. 2). We use these segments and glue parts as units when we extend the lattice, and call them *columns*. We always connect lead lines to a 0-grid segment.

The recursion formula of the site Green functions is obtained as follows. Consider a case of a finite scatterer with $l-1$ columns connected only to the left lead line, and add the lth column on the right side of the scatterer (see Fig. 2). By this extension, the Green function at the far right column G^L is transformed according to the following Dyson equation:

$$G^L(l) = [E - H_l - {}^tB_{l-1}G^L(l-1)B_{l-1}]^{-1} , \tag{2.8}$$

where H_l is the Hamiltonian inside the lth column and B_{l-1} is the one between the lth and $(l-1)$th columns. Therefore we can calculate $G^L(1), G^L(2), \ldots, G^L(l)$ by applying the recursion formula (2.8) successively starting from $G^L(0)$. Since the starting point $G^L(0)$ is the Green function of a square lattice with a finite width G_S, the analytic form is easily obtained for arbitrary complex energies. It should be noted that compared with the original

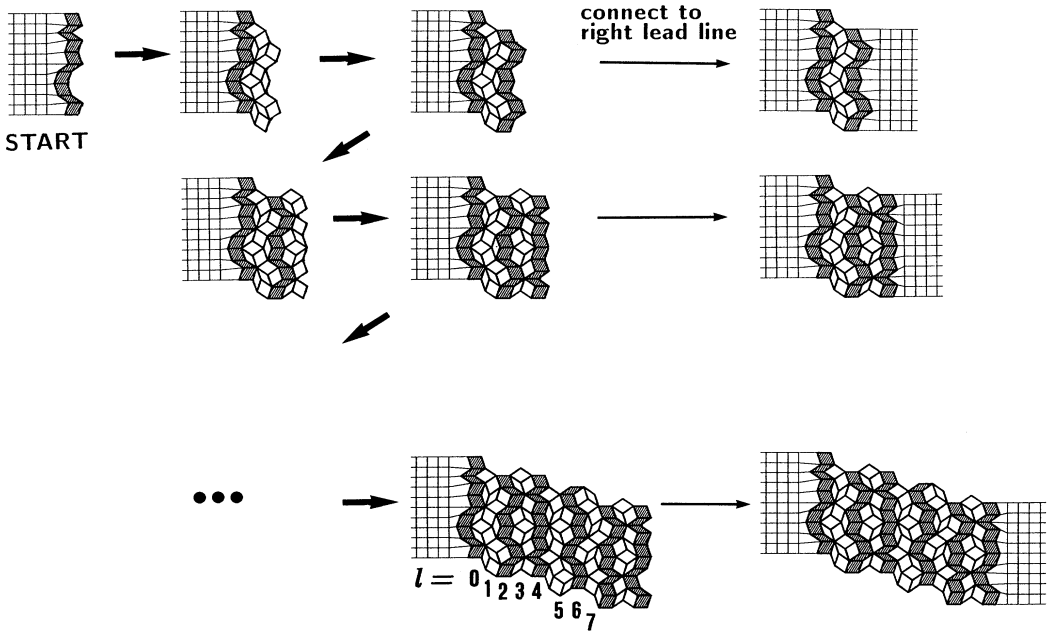

FIG. 2. Scheme of the recursion formula. The SPPL is being extended with recursion step and the configuration for the MCLF is provided by connecting it to the right lead line. The 0 grid in the SPPL is shaded.

one[14] the recursion relation used here has two different points due to its nonperiodic lattice structure. One is that the dimension of G^L, which equals the site number in the column, varies from column to column. The site number in the glue parts in the scatterer is on average 1.5 times that in the 0-grid segments, i.e., $1.5M$. The other difference is the irregular intercolumn transfer process, which is shown by the rectangular matrix B_{l-1}.

We can also obtain the Green functions G after we connect the above semi-infinite system to the right lead line using the Dyson equations:

$$G(l,l)=[E-H_l-G_S-{}^tB_{l-1}G^L(l-1)B_{l-1}]^{-1}\ , \quad (2.9a)$$

$$G(l+1,l+1)=[E-H_{l+1}-G_S-G^L(l)]^{-1}\ , \quad (2.9b)$$

$$G(l,l+1)=-G(l,l)G_S\ , \quad (2.9c)$$

where G_S again denotes the Green function of the semi-infinite square lattice. The conductance of the scatterer with l columns is given by inserting these Green functions into the definition (2.6).

This recursion method is very efficient. One advantage is that the dimensions of the matrices which we are manipulating are only the site numbers of each column (fewer than 1500 in our calculation), much smaller than the total site number in the scatterer (up to about 1.32 million). This method is hence particularly efficient for long scatterers. Another point is that while we are extending the scatterer conductance can be calculated at each length. For these reasons the recursion method is appropriate for studying length dependence.

III. ENERGY DEPENDENCE OF CONDUCTANCE

We show the energy dependence of conductance of the PL in Fig. 3. Using the direct method of the MCLF explained in the preceding section, we have calculated the conductance for five systems—the unit cells of PPL with

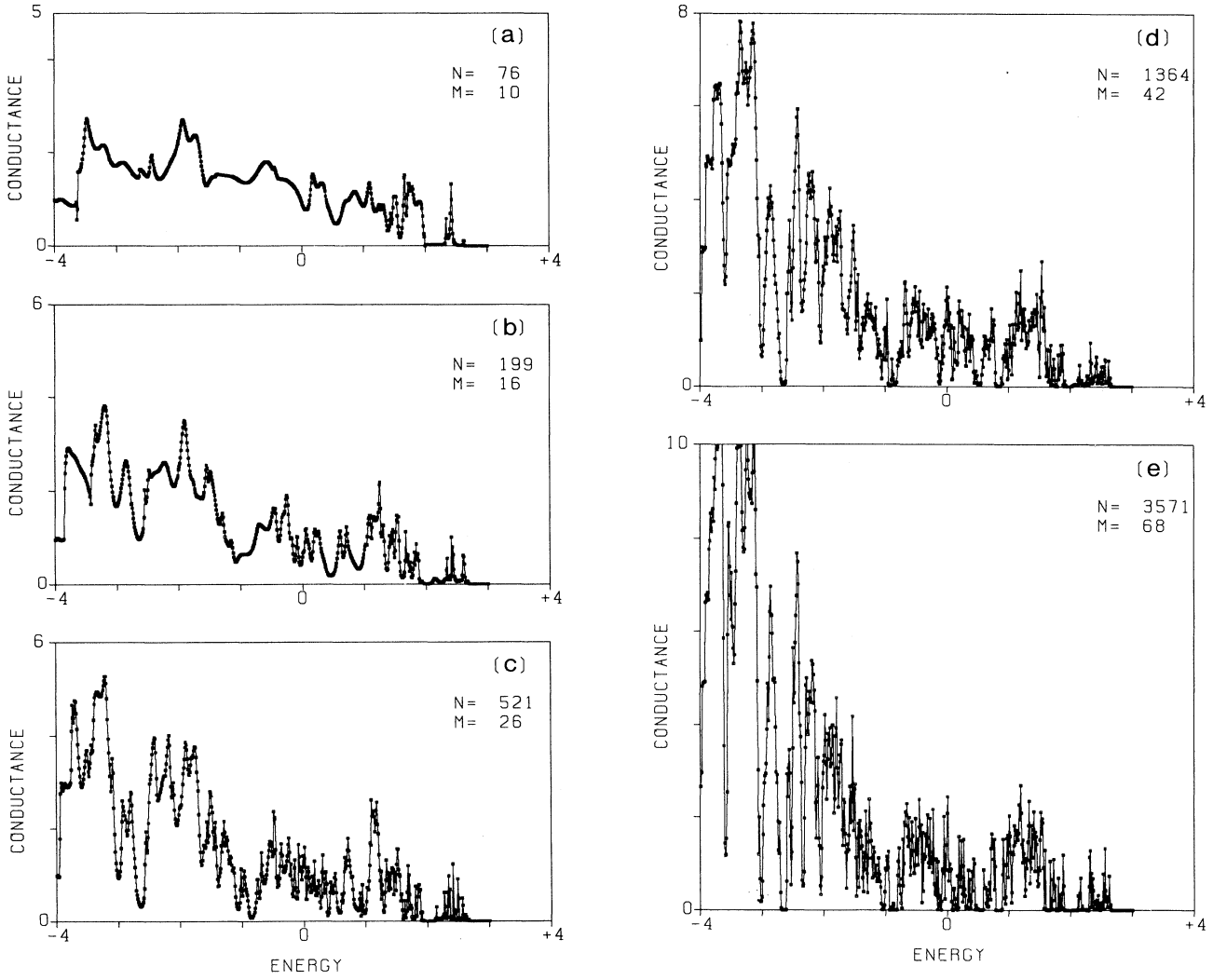

FIG. 3. Fermi-energy dependence of conductance for the unit cells of the PPL. Energy resolution is $\frac{1}{100}$.

the lattice widths $M=10,16,26,42,68$ and the site numbers $N=76,199,521,1364,3571$, respectively. The energy resolution of the curves is 0.01. We will focus on two features of the curves, conductance fluctuation with respect to the Fermi energy in each system and system-size dependence of this conductance fluctuation. We will compare the results with the electronic structure of the PL studied in Paper I, particularly by calculating the Thouless number.[18]

First, we notice that the conductance curves show large and rapid fluctuations with respect to the Fermi energy. This behavior contrasts with finite periodic systems such as a square lattice with a uniform on-site potential, which show smoother conductance curves. Second, the behavior of the conductance fluctuation strongly depends on energy regions. The conductance curves are relatively smooth at low energies, but very spiky at high energies.

This spiky conductance curve correlates with the unsmooth energy spectrum of the PL. We found by analyzing level statistics that the DOS has a singular part and the smoothness depends on the energy. As shown in Fig. 3 in Paper I, the DOS is much smoother in low-energy regions than in high-energy regions. The spiky conductance curves and strong energy dependence of conductance fluctuation can be interpreted mainly by these DOS behaviors. This interpretation is confirmed by the calculation of the Thouless number,[18] using the eigenenergies obtained in Paper I. The Thouless number is defined by the ratio of energy shift δE to energy separation ΔE, $g_{\mathrm{TH}}=\delta E/\Delta E$, δE being caused by modification of the boundary condition. The energy shifts δE measure the degree of localization of the wave functions, while $1/\Delta E$ means the DOS in a conventional sense, but the smoothness of the DOS is also involved in this term in our case. The Thouless number calculated for the PPL is shown in Fig. 4. Here, we define δE as the difference between maximum and minimum energies calculated in Paper I under four boundary conditions for a specified state, and define ΔE by the average energy separation between the specified state and the two neighboring states (each separation is also averaged over the four boundary conditions). Figure 4 shows the Thouless number with respect

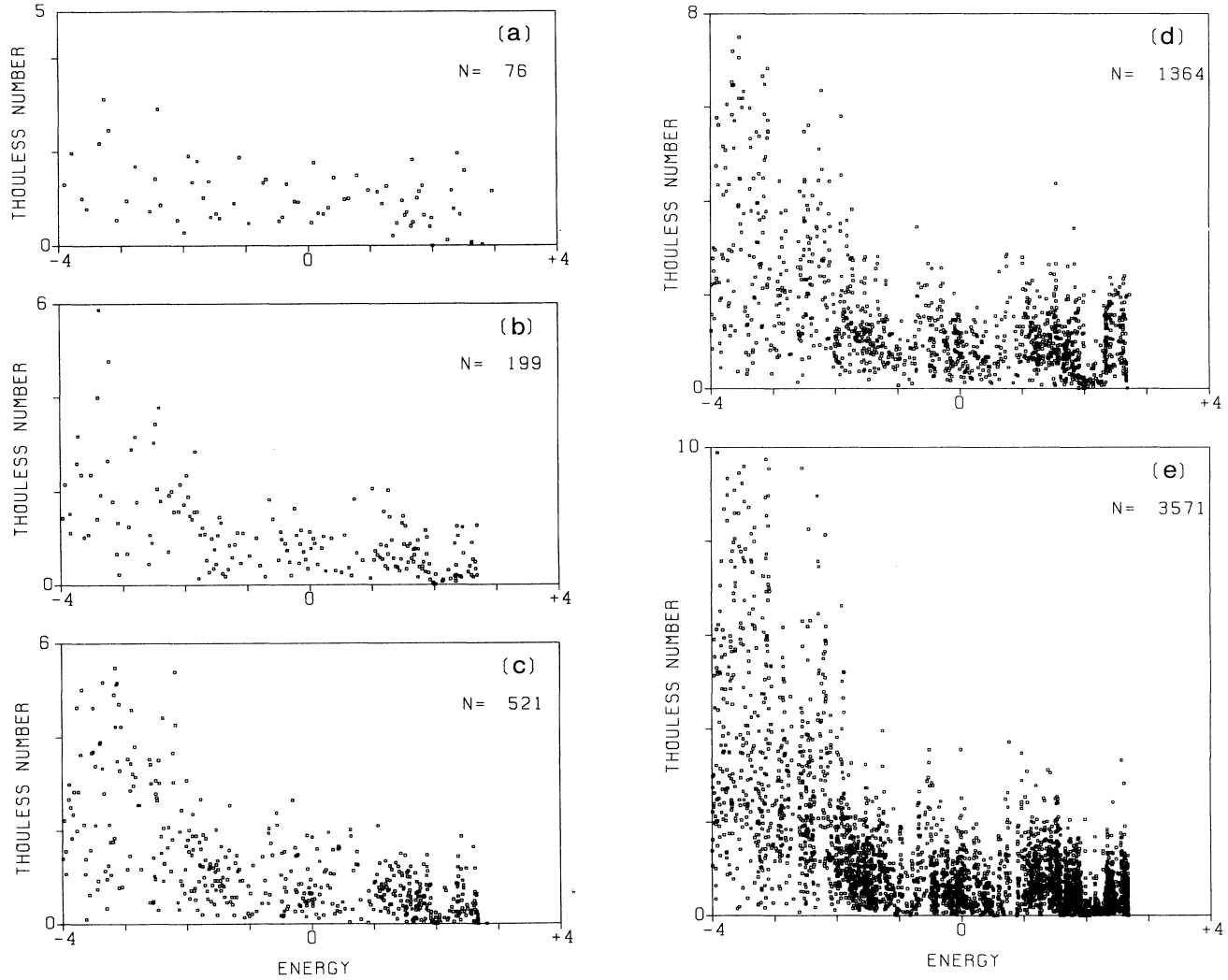

FIG. 4. Thouless number vs eigenenergy for all the eigenstates of the PPL.

to the eigenenergy averaged over the four boundary conditions, for all eigenstates of five PPL. This figure looks very similar to the conductance-energy curve in Fig. 3. This similarity means that the spiky behaviors of the conductance curves originate from the singular electronic structure, unsmooth DOS and critical wave functions.

The conductance curves show prominent dips at some energies, e.g., around $E=-2.65,-0.90,0.80,1.95$. These dips are caused by energy gaps in the DOS, which we can find clearly in Fig. 3 in Paper I. Since the dip structure becomes clearer with increasing system size, we believe that the gaps exist in the thermodynamic limit, although their origin is not well understood.

Next, we investigate the system-size dependence of this large fluctuation in the conductance-energy curves. Since the conductance fluctuation changes its behaviors depending on energy regions, we divide the total energy region into five subregions and calculate the average value and the standard deviation for each of the five PPL. The subregions are defined simply by the energy gaps in the DOS:[19] $E=(A)-4.00$ to -2.69, $(B)-2.61$ to -0.95, $(C)-0.82$ to 0.78, (D) 0.88 to 1.92, (E) 1.98 to 2.68. Figure 5 shows the averages and the standard deviations of the fluctuating conductance within these five energy regions calculated for five PPL. Later, we will show a more detailed result with a finer energy resolution for the largest system $N=3571$, which confirms the validity of this analysis.

As seen in Fig. 5, the conductance fluctuation changes in system-size dependence from low- to high-energy regions. This fact coincides with the result of diagonalization of the Hamiltonian wherein eigenfunctions change their spatial form depending on energy regions. In region A, the average increases with the system size, while the changes in regions $C-E$ are small. The behavior in region A is similar to the periodic system with extended wave functions, where the conductance is proportional to the channel number M, and this point will be made clear by studying length dependence later. On the other hand, the behaviors in the other regions indicate that the wave functions are not totally extended but rather localized. But those behaviors are also different from strongly localized systems, because strongly localized systems must show exponential decrease of the average and the fluctuation with the system size. In this sense, the conductance behaviors except in very low energy region are consistent with our conclusion that most wave functions in the PL are critical. Those behaviors are similar to the metallic systems with mesoscopic length scale, and it is interesting that the conductance fluctuation in the PL is the order of unity in units of e^2/h except at very low (A) and high (E) energy regions, which reminds us of the universal conductance fluctuation in mesoscopic systems.[20]

The two different behaviors of conductance were found earlier in another quasiperiodic model, the two-dimensional Fibonacci lattice (2D FL).[21] The 2D FL is a square lattice where the on-site potential is quasiperiodically distributed in the coordinate space. This model changes the character of electronic properties depending on the potential strength V. When V is small, the total bandwidth is finite and the conductance is large. On the other hand, when V is large, the total bandwidth is zero and the conductance is small and its fluctuation is the order of unity. Thus the behaviors in low- and high-energy regions of the PL are similar to the weak and strong potential cases of the 2D FL, respectively.

We show in Fig. 6 the conductance curve for the largest system $N=3571$ with a very fine energy resolution 0.0002. This resolution is fine enough to reproduce all fine structures of the curve. The statistics of conductance calculated for this result is also shown in Fig. 5, and this is coincident with the previous result calculated at a smaller number of energy points. The agreement confirms quantitative validity of our statistical treatment.

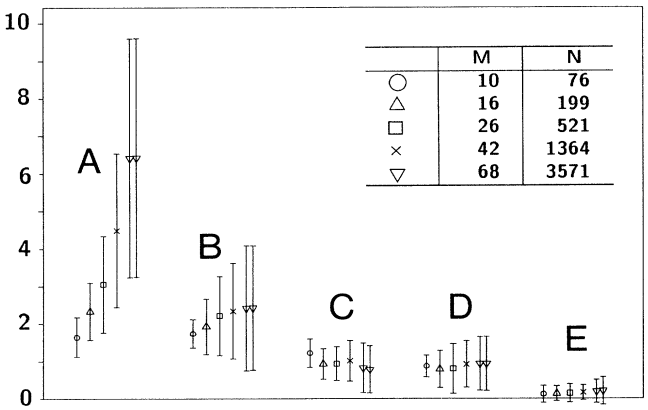

FIG. 5. Statistics of conductance for the PPL within five energy regions: $E=(A)$ -4.00 to -2.69, (B) -2.61 to -0.95, (C) -0.82 to 0.78, (D) 0.88 to 1.92, (E) 1.98 to 2.68. Center symbols show the averages, and half widths of the bars indicate the standard deviations. Data at far right in each energy region show the results for the energy resolution $\frac{1}{5000}$.

IV. LENGTH DEPENDENCE OF CONDUCTANCE

In this section we study the length dependence of conductance of the PL in extremely large systems and discuss the localization problem of the wave functions. For studying length dependence, the SPPL are more appropriate than the PPL used in the preceding section, because the SPPL hold quasiperiodicity in one direction. We consequently calculate conductance with extending the lattice in this quasiperiodic direction and fixing the lattice width. The lattices we use are the SPPL with a width of $M=68-752$ and a site number up to 1 318 368. From now on, we define the length of a SPPL by the ratio of the site number of the lattice to the lattice width, $L\equiv N/M$.

We will compare the length dependence of the conductance between low- and high-energy regions. Accordingly, we set the Fermi energy at some typical energies judging from the result of the energy dependence of the conductance. Magnified conductance curves in these two regions are shown in Fig. 6.

First, we consider the very low energy case. Figure 7 shows the result of length dependence at the Fermi ener-

gy $E=-3.90$. The curves are flat with small fluctuation as a function of the lattice length. This behavior indicates that the wave functions at this energy are almost freely extended like periodic systems, and this is consistent with the energy dependence. Below the energy $E=-3.80$, the conductance shows a stepwise curve as a function of the Fermi energy and the step values agree with the number of propagating plane waves (open channels) in the lead lines at each energy. Small fluctuation is the result of quantum resonance observed in finite systems. Therefore we conclude that the wave functions of the PL are extended, at very low energies, at least up to the maximum size we used.

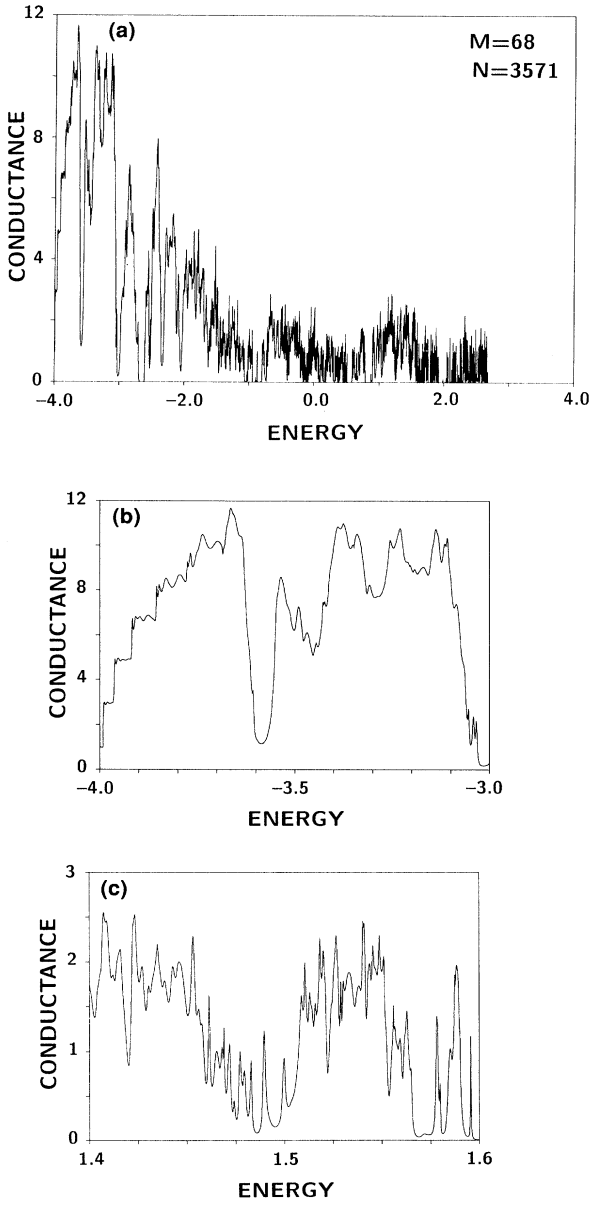

FIG. 6. Detailed energy dependence of conductance for the PPL with $N=3571$: (a) whole region, and magnified parts of (b) low- and (c) high-energy regions. Energy resolution is $\frac{1}{5000}$.

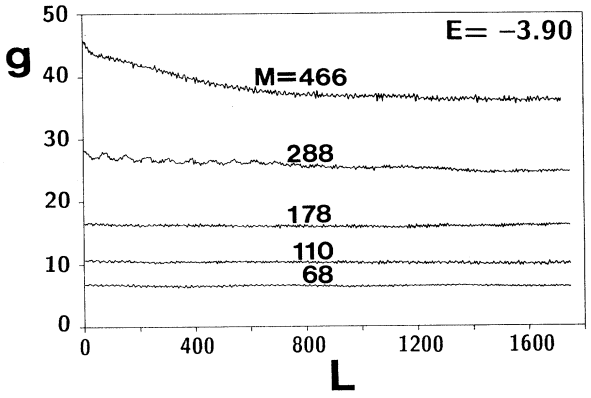

FIG. 7. Dependence of conductance for the SPPL on the length $L=N/M$ at a very low energy $E=-3.90$.

This length dependence seems inconsistent with our conclusion in Paper I that most of the wave functions are localized in a power law, but great care is necessary in its interpretation. First, we note that even though the wave functions may be extended in the very low energy region, this is not necessarily incompatible with the previous conclusion, because the previous conclusion was based on the distribution function of 8 norms; consequently, we cannot rule out the possibility that there still exist a very few extended wave functions since the 8-norm distribution is a statistical analysis. The second, and more plausible, possibility is that these extended behaviors might be the result of a finite-size effect and the wave functions will show power-law localizations in the limit of $M\rightarrow\infty$. The result of direct diagonalization of the Hamiltonian as well as the above length dependence shows the wave functions in the very low energy region can be well approximated by plane waves. This means that the wave functions do not "feel" the scattering potential before the scatterer reaches the size where quasiperiodicity is established in the length scale of wavelength of the corresponding plane wave. Since the wavelength becomes longer with decreasing energy, it is necessary to manipulate very large systems in order to estimate the thermodynamic behavior. In this sense, our calculation at $E=-3.90$ may not yet reach the size to show asymptotic behaviors, and it is possible to consider the slight decay part of the length dependence observed in the largest system, $M=466$, as precursor of a power-law localization. The system size used here is almost the upper limit in numerical computations. Of course, it is desirable to find an analytical treatment for the asymptotic behaviors, but we have not yet succeeded. One reason for the difficulty is that there is no continuous mapping that transforms the topologically "disordered" PL into a regular lattice, which forbids a conventional perturbative approach to this problem.

Next we consider a low-energy region, a bit higher than the previous case, where the conductance curve loses its stepwise character. Figure 8(a) shows the length dependence at $E=-3.40$ as an example. At this energy the conductance decreases slowly with the lattice length, and the log-log plot clearly shows a power-law decay [see

Fig. 8(b)]. The exponent of the power-law decay has not converged yet within our calculation but it is around 0.3 and hence we may expect the wave functions to be power-law localized in the thermodynamic limit.

We can confirm this power-law localization in some aspects. First, remember that finite parts of a SPPL with a specified size cannot be determined uniquely and there are a number of variations which correspond to the choice of the initial phases specified by the grid parameters $\{\gamma_j\}$ under the restriction $\sum_j \gamma_j = 0 \pmod 1$. We may consider them as different samples with the same structural properties. We calculate the conductance for several samples at the same energy in order to confirm that the power-law decay is an intrinsic property of the PL, not sample specific. The length dependence calculated for seven independent parts of the SPPL actually shows that the sample dependence of the power-law exponents is small at each lattice width (see Fig. 9). Another evidence is the result calculated at a nearby energy $E = -3.50$ shown in Fig. 10. At this energy the log-log plot again indicates that the conductance decay follows a power law. Thereby we conclude that the conductance shows power-law decays with respect to the lattice length in the low-energy region except in the very low energy part where the conductance-energy curve is stepwise.

Now we will discuss the absolute values of the power-law exponents, since the present results are small compared to those obtained in Paper I. As shown in Figs. 8 and 10, the exponents are 0.2–0.3; on the other hand, we

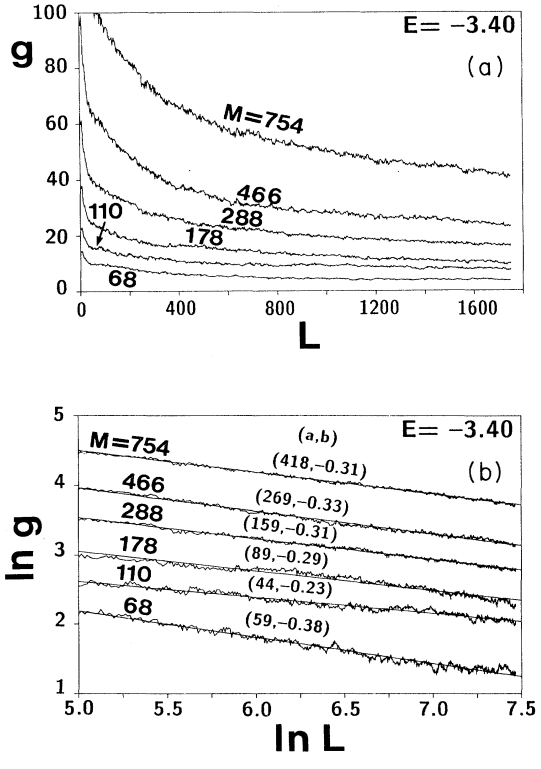

FIG. 8. (a) Length dependence of conductance at $E = -3.40$, and (b) its log-log plot. The least-squares fittings with $g(L) \sim aL^{-b}$ are superimposed in (b).

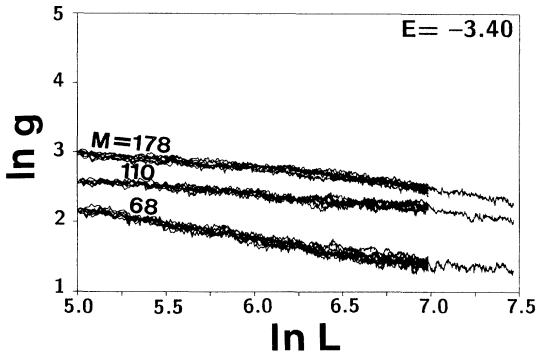

FIG. 9. Sample dependence of conductance decays. The results of seven other parts up to $L \sim 1000$ are superimposed on the curves shown in Fig. 8 for the smaller three SPPL.

concluded that most of the exponents are distributed from $\frac{3}{8}$ to $\frac{5}{8}$ based on the analysis of the 8 norm of the eigenfunctions. We believe that the discrepancy arises from the finite-size effect. Remember that all the eigenfunctions except the ground state have nodes and their amplitudes are small around the nodes. Therefore, if the lattice size is not sufficiently large in comparison with the length scale characterizing the sign change of the wave functions, the analysis of $2p$ norms is affected by the small-amplitude regions and it gives a larger exponent than the real value, which describes the power-law localization of the wave-function envelope. To determine the actual spatial form of the wave functions, we obtained the eigenfunction closest to the energy $E = -3.40$ for a fairly large system with $M = 68$ and $N = 39\,603$. The calculation was performed using the Lanczos method under the periodic boundary conditions, and energy of the obtained eigenstate was $E = -3.399\,51$. The eigenfunction revealed a complicated spatial structure with many nodes (characteristic length scale of sign change is about 8–20), and its charge-charge correlation function exhibits a self-similar structure. Hence the scatterer used for the 8-norm analysis ($M = 68$ and $N = 3571$) was not sufficiently large judging from the observed node density, and the 8-norm analysis must have given larger exponents including the finite-size correction. It should be noted that, in the length dependence of conductance presented above,

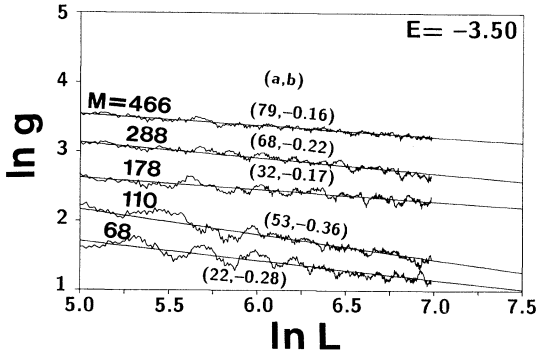

FIG. 10. Length dependence of conductance at another low energy $E = -3.50$.

the reason the smooth power-law behavior was observed rather than the self-similar behavior was that the self-similar structure was smeared out by the mixing of the open channels and the length dependence was dominated by the exponent of the wave-function envelope.

The analysis at high energies is much more difficult. For example, the length dependence at $E=1.50$ shown in Fig. 11 reveals faster decrease and larger conductance fluctuation than low-energy cases,[22] but we cannot so simply conclude that the wave functions are strongly localized and must take great care in the interpretation. As discussed in Paper I and as the energy dependence of conductance indicates, there exist many tiny energy gaps in the high-energy region and the DOS is more singular there than in the low-energy region, increasing with the system size. We hence cannot rule out the possibility that the specified Fermi energy may go out of the energy spectrum and drop into an energy gap while we are extending the lattice, and the observed fast conductance decay would be the result of this energy gap. In fact, another result in the high-energy region at $E=1.54$ shows the length dependence which looks like power-law decays (see Fig. 12).[23] The conductance-energy curve in Fig. 6(c) suggests that the energy $E=1.50$ is near an energy gap since the value of conductance is small, and in that case the observed length dependence is reasonable.

Finally, we mention an important scattering mechanism in topologically "disordered" systems. In Fig. 13 we show the simplest tight-binding model with a defect in the sense of topology. Since this model has a mirror symmetry in the vertical direction, the channels in the lead lines are classified into bonding and antibonding modes depending on the vertical momentum. The important fact is that an incident wave of the antibonding mode is perfectly reflected at the defect site and this perfect reflection does not depend on the energy of the incident wave. The origin of the perfect reflection is a topological "disorder," strictly speaking, change of the number of the sites through which the wave front passes, and so we will call it *topological scattering*. The PL have this property in their lattice structure, e.g., the ring statistics of our model ranges from 3 to 7 membered rings. Therefore the scattering mechanism of transport properties is essentially dominated by the topological scattering, and this

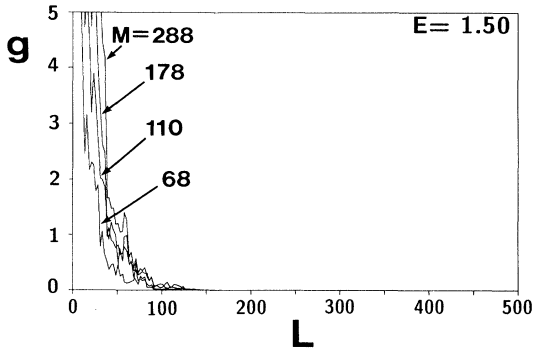

FIG. 11. Length dependence of conductance at a high energy $E=1.50$.

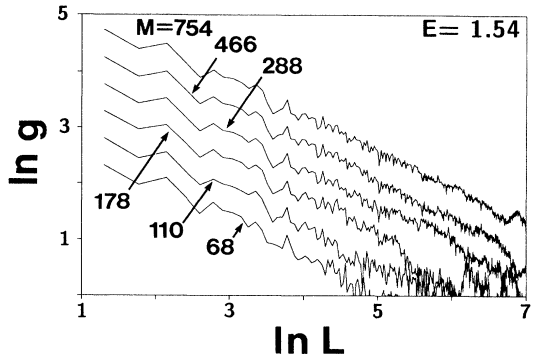

FIG. 12. Length dependence of conductance at another high energy $E=1.54$.

would be the origin of high resistivity.

The inapplicability of the transfer-matrix method mentioned in Sec. II stems from the topological scattering. Since some of the incident modes are perfectly reflected, the amplitudes of the wave functions on the right side [$\mathbf{a}_R$ and $\mathbf{b}_R$ in Eq. (2.1)] are not determined uniquely by those on the left side ($\mathbf{a}_L$ and $\mathbf{b}_L$), and consequently we cannot define the transfer matrix in principle. But the scattering problem is still well defined and there is no problem with our method.

V. CONCLUSION

In this paper we studied conductance of the PL as a function of the Fermi energy and the lattice length at zero temperature. The systems used in our calculations were five unit cells of PPL for studying the energy dependence up to the size of the lattice width $M=68$ and the site number $N=3571$, and SPPL for the length dependence up to $M=754$ and $N=1\,318\,368$. We used a tight-binding model where an s-like atom is sitting on the center of every rhombus and electron transfer energies are taken to be -1 only between nearest-neighbor rhombus pairs. In our calculations we applied the multichannel Landauer formula as the definition of conductance, and used the Lee-Fisher recursion method particularly in the study of the length dependence.

The results of the energy dependence show some characteristic features. We found that the conductance curves are very spiky with respect to the Fermi energy and the degree of this spiky character depends on the energy region. The conductance curve takes large values and it is relatively smooth at low energies, but very spiky at high energies. These behaviors can be explained by the character of the energy spectrum studied in Paper I. From the analysis of level statistics and approximated band calculation, we found that the energy spectrum of

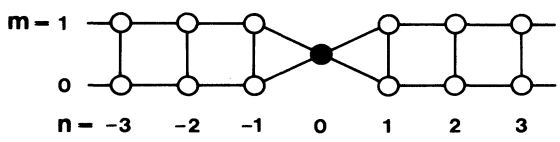

FIG. 13. A simple example of the topological scattering. The topological defect site is shown by the solid circle.

the PL has an unsmooth part and that the unsmoothness increases with the system size and depends on energy regions, i.e., it is more spiky in high-energy regions. We therefore think that the unsmooth spectrum character directly results in spiky conductance-energy curves of the PL, and this relationship is explicitly visualized by the energy dependence of the Thouless number. The fluctuations in the conductance-energy curves reveal only small system-size dependence except in very low energy region, both in their averages and standard deviations. This system-size dependence is different from freely extended systems and strongly localized systems, which is consistent with our previous conclusion that most of the wave functions are critical, and we reexamined this point through a more direct analysis, length dependence of the conductance. The observed fluctuations in the order of unity have similarity with the universal conductance fluctuation in mesoscopic systems.

The length dependence shows power-law decays of the conductance except at very low energies. Since the length dependence of conductance exhibits the character of the wave functions in the coordinate space, these results support that the wave functions of the PL are critical. We should mention that other behaviors are also observed in the length dependence. One example is that the conductance does not decay but only fluctuates at very low energies. This behavior indicates that the wave functions are extended as in periodic systems, and is consistent with the stepwise behavior in the energy dependence in this energy region. But further study is necessary to answer the question of whether this extended character would be intrinsic or not, i.e., an effect of finite system size. The other example is fast conductance decay observed at some high energies, but we do not think this fast decay is intrinsic since it could be interpreted by a gap formation in the energy spectrum at a specified Fermi energy by extending the lattice. As a matter of fact, the conductance shows power-law decays when the energy is shifted slightly higher.

As discussed above, our previous conclusion that most of the wave functions are critical was convincingly supported in the qualitative sense by the present result that the conductance showed power-law decays at most energies. Nonpower behaviors observed at some energies can be explained as the result of extrinsic factors, and we may hence consider them as exceptional cases. However, there is a quantitative discrepancy in the power-law exponents; the present result gave exponents smaller than those given by the analysis of 8 norms in Paper I. By examining the applicability of the 8-norm analysis, we found that the finite-size effect is not negligible at low energies and the 8-norm analysis gave exponents larger than the real values in our calculation. Therefore we believe that more reliable exponents are the present results determined from the length dependence of conductance.

In summary, conductance of the PL is characterized by spiky energy dependence and power-law decays with the lattice length. The spiky behaviors in the energy dependence correspond to the unsmooth DOS of the PL and the power-law decays originate from the wave functions localized in a power law. These transport properties are dominated by the strong scattering due to topological nonperiodicity in the lattice structure.

ACKNOWLEDGMENTS

The authors thank Takeo Fujiwara for providing his program for generating PPL. This work was supported by a Grant-in-Aid for Scientific Research on Priority Areas, "Quasicrystals," from the Ministry of Education, Science and Culture of Japan.

[1]H. Tsunetsugu, T. Fujiwara, K. Ueda, and T. Tokihiro, preceding paper, Phys. Rev. B **43**, 8879 (1991), referred to as Paper I.

[2]H. Tsunetsugu, T. Fujiwara, K. Ueda, and T. Tokihiro, J. Phys. Soc. Jpn. **55**, 1420 (1986).

[3]H. Tsunetsugu and K. Ueda, Phys. Rev. B **38**, 10 109 (1988).

[4]H. Tsunetsugu, J. Non-Cryst. Solids **117/118**, 781 (1990).

[5]H. Tsunetsugu, in *Quasicrystals,* Proceedings of the 12th Taniguchi Symposium, Shima, 1989, edited by T. Fujiwara and T. Ogawa (Springer, Berlin, 1990).

[6]T. C. Choy, Phys. Rev. B **35**, 1456 (1987).

[7]J. B. Sokoloff, Phys. Rev. Lett. **57**, 2223 (1986).

[8]P. W. Anderson, D. J. Thouless, E. Abrahams, and D. S. Fisher, Phys. Rev. B **22**, 3519 (1980).

[9]For example, J. Kollár and A. Sütö, Phys. Lett. A **117**, 203 (1986); P. Hu and C. S. Ting, Phys. Rev. B **34**, 8331 (1986); T. Schneider, A. Poloti, and D. Würtz, Z. Phys. B **66**, 469 (1987); S. D. Sarma and X. C. Xie, Phys. Rev. B **37**, 1097 (1988).

[10]B. Sutherland and M. Kohmoto, Phys. Rev. B **36**, 5877 (1987).

[11]M. Goda, J. Phys. Soc. Jpn. **56**, 1924 (1987).

[12]M. Kohmoto, L. P. Kadanoff, and C. Tang, Phys. Rev. Lett. **50**, 1870 (1983); S. Ostlund, R. Pandit, D. Rand, H. J. Schellnhuber, and E. D. Siggia, *ibid.* **50**, 1873 (1983).

[13]Y. Imry, Europhys. Lett. **1**, 249 (1986).

[14]P. A. Lee and D. S. Fisher, Phys. Rev. Lett. **47**, 882 (1981).

[15]A. MacKinnon and B. Kramer, Z. Phys. B **53**, 1 (1983).

[16]P. W. Anderson, Phys. Rev. B **23**, 4828 (1981); M. Ya Azbel, J. Phys. C **14**, L225 (1981); M. Büttiker, Y. Imry, R. Landauer, and S. Pinhas, Phys. Rev. B **31**, 6207 (1985), and references therein.

[17]K. Semba, Master's thesis, Tokyo University (1985); K. Semba and T. Ninomiya (private communication); T. Fujiwara, M. Arai, T. Tokihiro, and M. Kohmoto, Phys. Rev. B **37**, 2797 (1988).

[18]D. J. Thouless, Phys. Rev. Lett. **39**, 1167 (1975).

[19]We change the range of region (E) from the previous one in Ref. 3, considering conductance almost vanishes above the band top of the energy spectrum.

[20]P. A. Lee and A. D. Stone, Phys. Rev. Lett. **55**, 1622 (1985); B. L. Al'tshuler, Pis'ma Zh. Eksp. Teor. Fiz. **41**, 530 (1985) [JETP Lett. **41**, 648 (1985)]; P. A. Lee, A. D. Stone, and H. Fukuyama, Phys. Rev. B **35**, 1039 (1987), and references therein.

[21]K. Ueda and H. Tsunetsugu, Phys. Rev. Lett. **58**, 1272 (1987).

[22]The results of $E=1.50$ presented in Refs. 4 and 5 were calculated on the same SPPL, but different parts were used there.

[23]Another high-energy result $E=1.52$ was presented in Ref. 5.